The mechanisms of electron acceleration in antiparallel and guide field magnetic reconnection

Can Huang,[1,2] Quanming Lu,[1,2,a)] and Shui Wang[1]
[1]*CAS Key Laboratory of Basic Plasma Physics, School of Earth and Space Sciences, University of Science and Technology of China, Hefei, Anhui 230026, China*
[2]*State Key Laboratory of Space Weather, Chinese Academy of Sciences, Beijing 100190, China*

(Received 1 April 2010; accepted 7 June 2010; published online 27 July 2010)

Two-dimensional particle-in-cell simulations are performed to investigate electron dynamics in antiparallel and guide field (in the presence of a strong guide field) magnetic reconnection, and the mechanisms of electron acceleration are compared. In the antiparallel reconnection, the dominant acceleration occurs in the vicinity of the X line, where the magnetic field is weak. Most of these electrons come from the regions just outside of the separatrices, which move into the vicinity of the X line along the magnetic field lines. Electrons can also be nonadiabatically accelerated in the pileup region by the reconnection electric field, where the gyroradii of the electrons are comparable to the curvature radii of the magnetic field lines. Most of these electrons come from the regions inside of the separatrices, which move into the pileup region along the magnetic field lines. In the guide field reconnection, electrons are accelerated by the parallel electric field. They are firstly accelerated when moving toward the X line along the magnetic field lines, and then are further accelerated when they are funneled into the vicinity of the X line. Most of energetic electrons come from the region outside of the pair of the negative separatrices. The efficiency of such an acceleration mechanism is obviously higher than that in the antiparallel reconnection. In both the antiparallel and guide field reconnection, the mechanisms of electron acceleration favor the electrons with higher initial energy. © *2010 American Institute of Physics*. [doi:10.1063/1.3457930]

I. INTRODUCTION

In collisionless plasma, magnetic reconnection provides a physical mechanism for fast energy conversion from magnetic energy to plasma kinetic energy,[1–6] which is used to explain the bursts in solar atmosphere, interplanetary space and the Earth's magnetosphere.[7–12] Such a conversion process is manifested by plasma heating and plasma jetting in the reconnection outflow regions. The structures of antiparallel and guide field (in the presence of a strong guide field) magnetic reconnection are found to be different: in antiparallel reconnection, both the out-of-plane magnetic field and electron flow are symmetric, and the out-of-plane magnetic field has a quadrupole structure;[13–16] in guide field reconnection, the out-of-plane magnetic field does not exhibit a quadrupole structure, and the structures of both the out-of-plane magnetic field and electron flow are substantially distorted.[16–18] However, energetic electrons are important signatures in both antiparallel and guide field reconnection. In solar flares, x ray is thought to be generated by the energetic electrons in magnetic reconnection.[19–21] In the Earth's magnetotail, there have been direct measurements of energetic electrons up to several hundreds of keV.[15,22–26] Energetic electrons are also seen during sawtooth crashes and disruptions in laboratory tokamak experiments.[27]

Recently, several authors have investigated electron acceleration in magnetic reconnection with self-consistent particle-in-cell (PIC) simulations. Hoshino *et al.*[28] studied electron acceleration in antiparallel reconnection, and found that electrons can be accelerated not only in the X-type region by meandering motions but also in the magnetic field pileup region by gradient and the curvature drift motions. Hoshino further demonstrated that the polarization electric field can be enhanced greatly in an externally driven antiparallel reconnection. Part of electrons may then be trapped and accelerated to high energy in the X-type region by utilizing surfing acceleration.[29] Pritchett[30] also studied electron acceleration in driven antiparallel reconnection, and demonstrated that the relativistic electrons can be easily produced. These electrons are considered to be dominantly accelerated in the vicinity of the X line by the inductive reconnection electric field when their velocity component in the x direction $v_x \approx 0$. Pritchett[31] also investigated electron acceleration in guide field reconnection. At first, a cold electron beam is formed along one pair of separatrices due to the parallel electric field that exists in the low-density cavities. The electron beam is funneled into the vicinity of the X line, and these electrons are then further accelerated by the parallel electric field. Drake *et al.*[32] suggested that electrons may gain energy in guide field reconnection by Fermi acceleration, where the electrons are reflected from the ends of the contracting magnetic islands. The influences of the guide field on acceleration were also discussed by Fu *et al.*[16] They demonstrated that electrons can be accelerated in both the X-type and O-type regions in antiparallel reconnection, while the obvious acceleration can only be observed in the X-type region in guide field reconnection. The energetic electrons in the O-type region of the antiparallel reconnection are nonadia-

a)Author to whom correspondence should be addressed. Electronic mail: qmlu@ustc.edu.cn.

 © 2010 American Institute of Physics

Downloaded 27 Jul 2010 to 211.86.159.15. Redistribution subject to AIP license or copyright; see http://pop.aip.org/pop/copyright.jsp

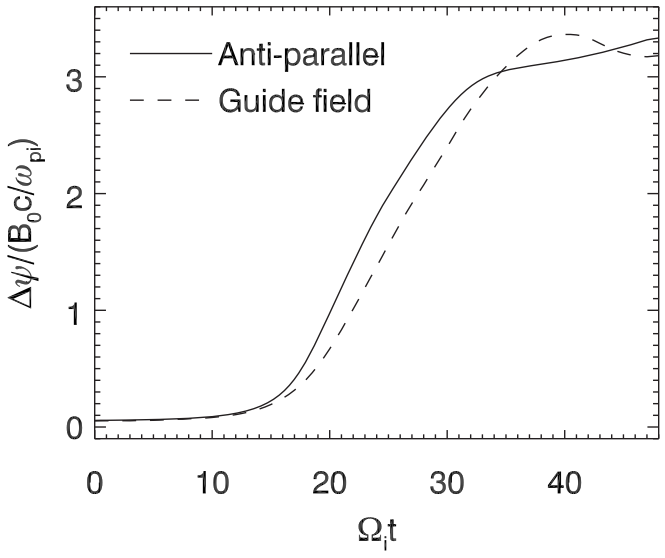

FIG. 1. Time history of the reconnection magnetic flux in the antiparallel (solid line) and guide field reconnection (dashed line).

batically accelerated when their gyroradii are comparable to the curvature radii of the magnetic field lines.[16]

In this paper, we perform two-dimensional (2D) PIC simulations to investigate electron dynamics in antiparallel and guide field reconnection. The mechanisms of electron acceleration in antiparallel and guide field reconnection are found to be quite different. At the same time, the influences of the electron initial positions/energy on the acceleration efficiency, as well as the formation mechanisms of different electron distributions in different regions, are also studied.

The paper is organized as follows. The simulation model is presented in Sec. II. The simulation results of electron dynamics in antiparallel and guide field reconnection are described in Sec. III. The conclusions and discussion are given in Sec. IV.

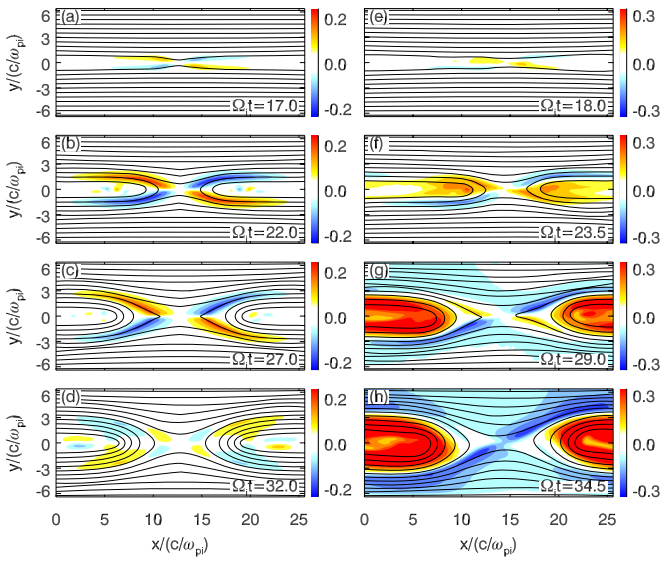

FIG. 2. (Color online) Representations of B_z/B_0 in the antiparallel reconnection at $\Omega_i t$=17, 22, 27, and 32 are presented in [(a)–(d)], respectively. Representations of $B_z'=(B_z-B_{z0})/B_0$ in the guide field reconnection at $\Omega_i t$ =18, 23.5, 29, and 34.5 are presented in [(e)–(h)], respectively. The solid lines in the figure represent the magnetic field lines.

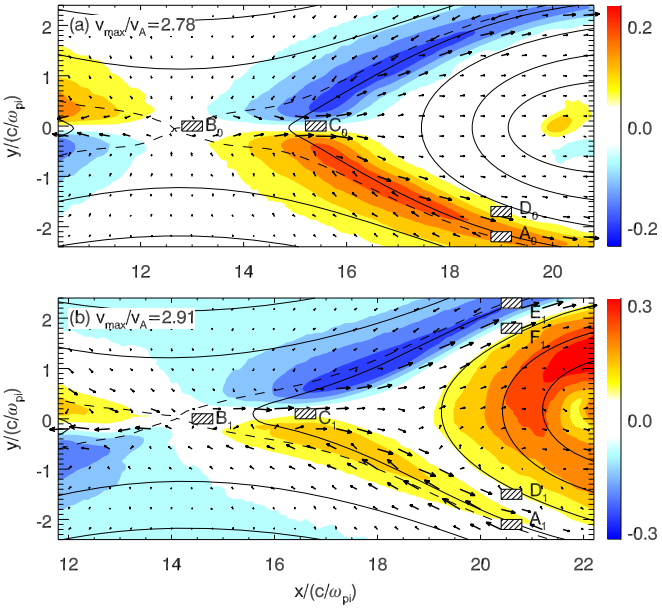

FIG. 3. (Color online) Electron flow vectors (black arrows) and magnetic field lines (black contours) in the x,y plane at $\Omega_i t$=27 and 29 for (a) antiparallel and (b) guide field reconnection, respectively. The magnitude of the out-of-plane magnetic field is also plotted.

II. SIMULATION MODEL

A 2D PIC simulation code is used in this paper to investigate the electron dynamics in both antiparallel and guide field magnetic reconnection. In the simulations, the electromagnetic fields are defined on the grids and updated by solving the Maxwell equations with a full explicit algorithm. In our simulation model, the initial configuration is a one-dimensional Harris current sheet in the (x,y) plane, and the initial magnetic field is given by

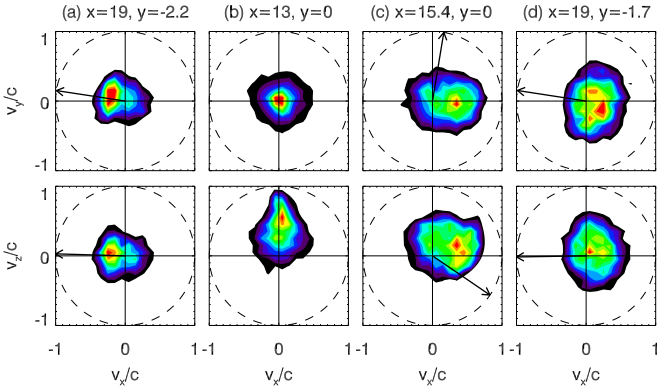

FIG. 4. (Color online) The electron velocity distributions $f(v_x,v_y)$ and $f(v_x,v_z)$ for the antiparallel reconnection at $\Omega_i t$=27 in different regions, whose centers are located at (a) $x=19c/\omega_{pi}$, $y=-2.2c/\omega_{pi}$; (b) $x=13c/\omega_{pi}$, $y=0$; (c) $x=15.4c/\omega_{pi}$, $y=0$; (d) $x=19c/\omega_{pi}$, $y=-1.7c/\omega_{pi}$, and the size is $0.4c/\omega_{pi}\times 0.2c/\omega_{pi}$. The arrows show the directions of the local magnetic field.

Downloaded 27 Jul 2010 to 211.86.159.15. Redistribution subject to AIP license or copyright; see http://pop.aip.org/pop/copyright.jsp

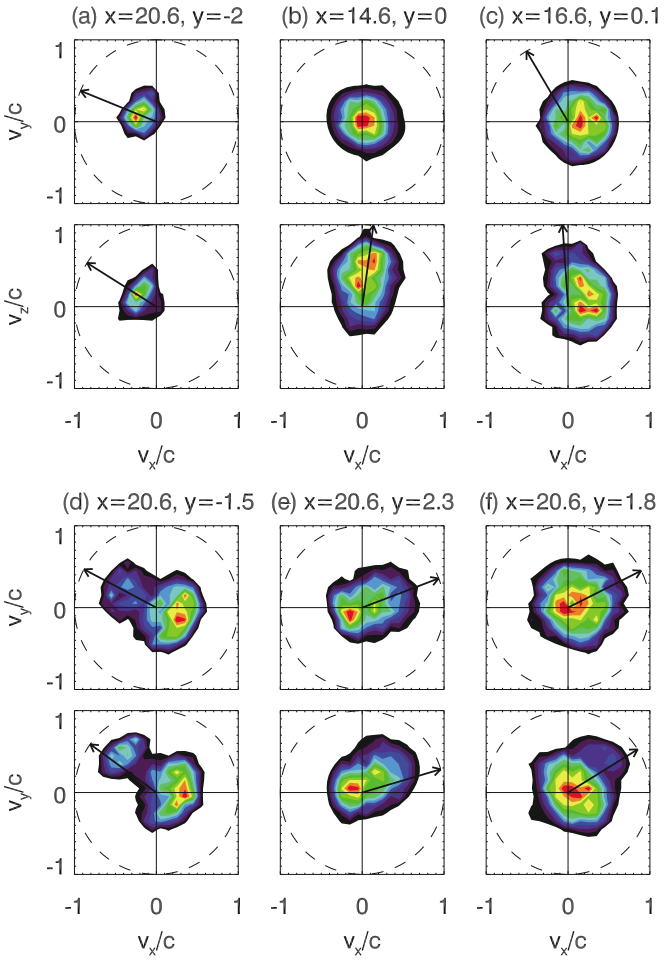

FIG. 5. (Color online) The electron velocity distributions $f(v_x,v_y)$ and $f(v_x,v_z)$ for the guide field reconnection at $\Omega_i t=29$ in different regions, whose centers are located at (a) $x=20.6c/\omega_{pi}$, $y=-2c/\omega_{pi}$; (b) $x=14.6c/\omega_{pi}$, $y=0$; (c) $x=16.6c/\omega_{pi}$, $y=0.1c/\omega_{pi}$; (d) $x=20.6c/\omega_{pi}$, $y=-1.5c/\omega_{pi}$; (e) $x=20.6c/\omega_{pi}$, $y=2.3c/\omega_{pi}$; (f) $x=20.6c/\omega_{pi}$, $y=1.8c/\omega_{pi}$, and the size is $0.4c/\omega_{pi}\times 0.2c/\omega_{pi}$. The arrows show the directions of the local magnetic field.

$$\mathbf{B}_0(y) = B_0 \tanh\left[\left(y-\frac{L_y}{2}\right)\Big/\delta\right]\mathbf{e}_x + B_{z0}\mathbf{e}_z, \tag{1}$$

where δ is the half-width of the current sheet, B_0 is the asymptotical magnetic strength, B_{z0} is the strength of the guide field, and L_y is the size of the simulation domain in the y direction. The corresponding number density is

$$n(y) = n_b + n_0 \operatorname{sech}^2\left[\left(y-\frac{L_y}{2}\right)\Big/\delta\right], \tag{2}$$

where n_b represents the density of the background plasma and n_0 is the peak Harris density. The distribution functions for the ions and electrons are Maxwellian, and their drift speeds in the z direction satisfy $V_{i0}/V_{e0}=T_{i0}/T_{e0}$, where $V_{i0}(V_{e0})$ and $T_{i0}(T_{e0})$ are the drift speed and initial temperature for ions(electrons), respectively. In our simulations, the temperature ratio is $T_{i0}/T_{e0}=4$, and $n_0=5n_b$. The current sheet width is $\delta=0.5c/\omega_{pi}$, where c/ω_{pi} is the ion inertial length defined by n_0. The mass ratio is set to $m_i/m_e=100$. The light speed is set to $c=15v_A$, where v_A is the Alfvén speed defined by B_0 and n_0.

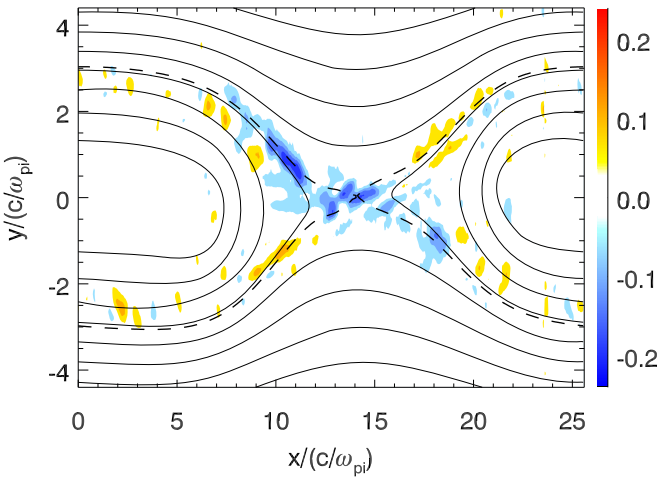

FIG. 6. (Color online) The parallel electric field at $\Omega_i t=29$ in the guide field reconnection. In the figure, the solid and dashed lines represent the magnetic field lines and separatrices, respectively.

The computation is carried out in a rectangular domain in the (x,y) plane with dimension $L_x\times L_y=(25.6c/\omega_{pi})\times(12.8c/\omega_{pi})$. An $N_x\times N_y=512\times 256$ grid system is employed in the simulations, so the spatial resolution is $\Delta x=\Delta y=0.05c/\omega_{pi}=0.5c/\omega_{pe}$. The time step is $\Omega_i t=0.001$, where Ω_i is the ion gyrofrequency. We employ more than 1.0×10^7 particles per species. The periodic boundary conditions are used along the x direction, while the ideal conducting boundary conditions for electromagnetic fields are employed in the y direction. In order to make the system enter the nonlinear stage quickly, an initial flux perturbation is introduced as follows, which is useful to reach the stage of rapid growth of reconnection rate

$$\psi(x,y) = \psi_0 \cos\left[2\pi\left(x-\frac{L_x}{2}\right)\Big/L_x\right] \times\cos\left[\pi\left(y-\frac{L_y}{2}\right)\Big/L_y\right]. \tag{3}$$

where ψ is the y component of the vector potential and ψ_0 is set to $\psi_0/(B_0c/\omega_{pi})=0.05$. The parameters and boundary conditions are based on in the geospace environment modeling (GEM) magnetic reconnection challenge with small modifications,[6] such as a larger ion-to-electron mass ratio.

III. SIMULATION RESULTS

In this paper, we perform 2D PIC simulations to investigate the mechanisms of electron acceleration in antiparallel and guide field reconnection, and their initial guide fields are $B_{z0}/B_0=0$ and $B_{z0}/B_0=0.5$, respectively. Figure 1 shows the time evolution of the reconnected magnetic flux $\Delta\psi$ in the antiparallel and guide field reconnection. Here the magnetic flux $\Delta\psi$ is defined as the flux difference between the X and O lines, and its slope can be served as an indicator for the magnetic reconnection rate. The reconnection rate in the guide field reconnection is slightly smaller than that in the antiparallel reconnection. The results are similar to the GEM challenge.[6]

Downloaded 27 Jul 2010 to 211.86.159.15. Redistribution subject to AIP license or copyright; see http://pop.aip.org/pop/copyright.jsp

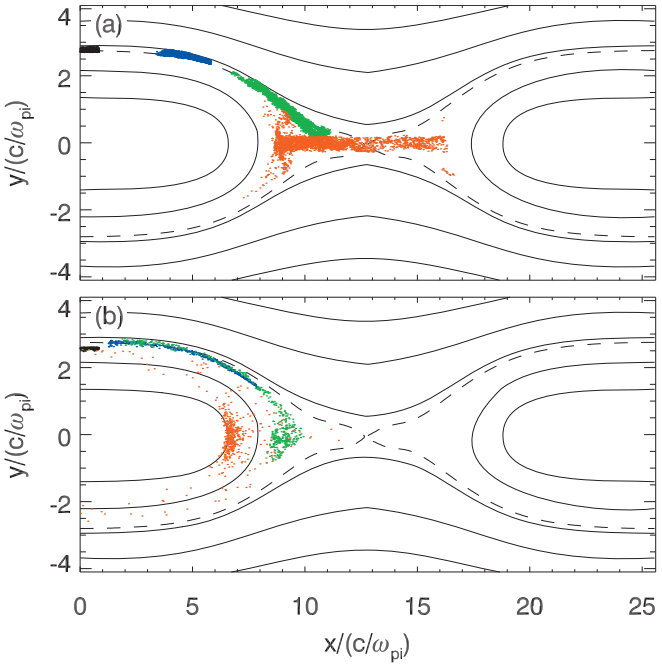

FIG. 7. (Color) The positions of test electrons at different times in the antiparallel reconnection, and the initial kinetic energy of the electrons is $0.1m_ec^2$. (a) Initially, the test electrons are located in the region $0<x<0.8c/\omega_{pe}$, $2.7c/\omega_{pi}<y<2.9c/\omega_{pi}$, just outside of the separatrix. The different color of the dots represents the positions of test electrons at different times. Black, blue, green, and red dots describe the positions of the test electrons at $\Omega_i t_1=0$, 0.8, 1.6, and 2.4, respectively. (b) Initially, the test electrons are located in the region $0<x<0.8c/\omega_{pe}$, $2.4c/\omega_{pi}<y<2.6c/\omega_{pi}$, just inside of the separatrix. The different color of the dots represents the positions of test electrons at different times. Black, blue, green, and red dots describe the positions of the test electrons at $\Omega_i t_1=0$, 1.2, 2, and 6, respectively. In the figure, only the particles with kinetic energy $\varepsilon>0.25m_ec^2$ are plotted, except for the particles in the initial time. The time t_1 is measured from $\Omega_i t=27$, when the fixed electric and magnetic field are taken.

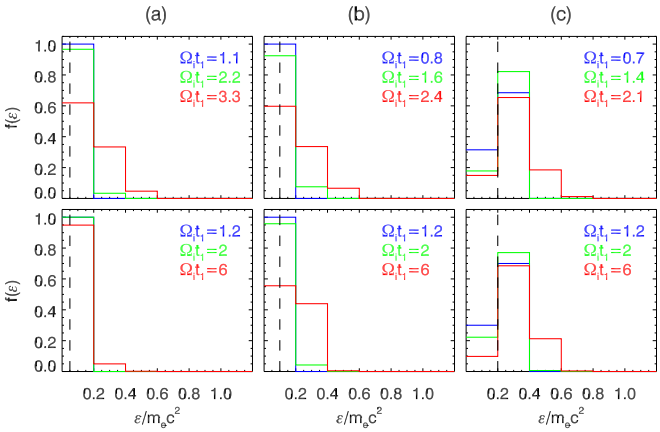

FIG. 8. (Color online) The electron energy distributions at different times in the antiparallel reconnection. In the top panel, the initial positions of the test electrons are located at the region $0<x<0.8c/\omega_{pe}$, $2.7c/\omega_{pi}<y<2.9c/\omega_{pi}$, just outside of the separatrix. In the bottom panel, the initial positions of the test electrons are located at the region $0<x<0.8c/\omega_{pe}$, $2.4c/\omega_{pi}<y<2.6c/\omega_{pi}$, just inside of the separatrix. (a), (b), and (c) represent the different electron energy, which are $0.05m_ec^2$, $0.1m_ec^2$, and $0.2m_ec^2$, respectively. In the figure, the initial kinetic energies are described with dashed lines, The time t_1 is measured from $\Omega_i t=27$, when the fixed electric and magnetic field are taken.

Figure 2 shows the time evolution of the out-of-plane magnetic field B_z/B_0 at $\Omega_i t=17$, 22, 27, and 32 in the antiparallel reconnection and $B_z'=(B_z-B_{z0})/B_0$ at $\Omega_i t=18$, 23.5, 29, and 34.5 in the guide field reconnection. The magnetic field lines are also plotted in the figure for reference. The left and right columns plot the out-of-plane magnetic field in the antiparallel and guide field reconnection, respectively. As time goes on, the width of the current sheet increases in both the antiparallel and guide field reconnection. The widths of the current sheet saturates at about $7c/\omega_{pi}$ and $8c/\omega_{pi}$ for the antiparallel and guide field reconnection, respectively. In the antiparallel reconnection, the out-of-plane magnetic field B_z/B_0 exhibits a quadrupole structure with the maximum amplitude about 0.2. Such a quadrupole structure is generally considered to be formed by the in-plane Hall current system. In the guide field reconnection, the out-of-plane magnetic field is substantially distorted, and it does not exhibit a quadrupole structure.

Figure 3 describe the in-plane electron flow in the antiparallel and guide field reconnection. The magnetic field lines, as well as the out-of-plane magnetic field, are also plotted in the figure. Figure 3(a) shows the electron flow vectors in the (x,y) plane at $\Omega_i t=27$ for the antiparallel reconnection, and Fig. 3(b) shows the electron flow vectors at $\Omega_i t=29$ for the guide field reconnection. In the antiparallel reconnection, the electron flow pattern is symmetric along the x axis. Consistent with observations,[25] an electron beam with lower velocity streams toward the X line along each separatrix, while an electron beam with higher velocity streams away from the X line along the magnetic field lines just inside of each separatrix. The electron beam toward the X line is caused by the magnetic mirror in the reconnection site, while the electron beam away from the X line is formed after the electrons are accelerated in the vicinity of the X line. The maximum velocity of the electron beam away from the X line is about $3v_A$. In the guide field reconnection, as indicated by Pritchett,[31] the symmetry of the electron flow pattern along the x axis is destroyed. Strong electron inflow beams toward to the X line can only be found along the pair of the negative separatrices (from the top-left corner to the bottom-right corner), while strong electron outflow beams can be observed along the magnetic field lines inside of the pairs of both the negative and positive separatrices (from the bottom-left corner to the top-right corner). The maximum velocity of the outflow electron beam is about $4.5v_A$, which is larger than that in the antiparallel reconnection.

Figure 4 shows 2D electron velocity distributions $f(v_x,v_y)$ and $f(v_x,v_z)$ at different regions in the antiparallel reconnection. The arrows in the figure show the directions of the local magnetic field. The results in (a)–(d) are obtained from the regions A_0-D_0 denoted in Fig. 3(a). In the region along the negative separatrix (denoted by A_0), there is an electron beam directed toward the X line along the magnetic field lines. The electron beam is formed due to the effect of the magnetic mirror, because the magnetic field is weak in the vicinity of the X line. After these electrons reach the vicinity of the X line (denoted by B_0), they are accelerated by the reconnection electric field and form an electron beam

Downloaded 27 Jul 2010 to 211.86.159.15. Redistribution subject to AIP license or copyright; see http://pop.aip.org/pop/copyright.jsp

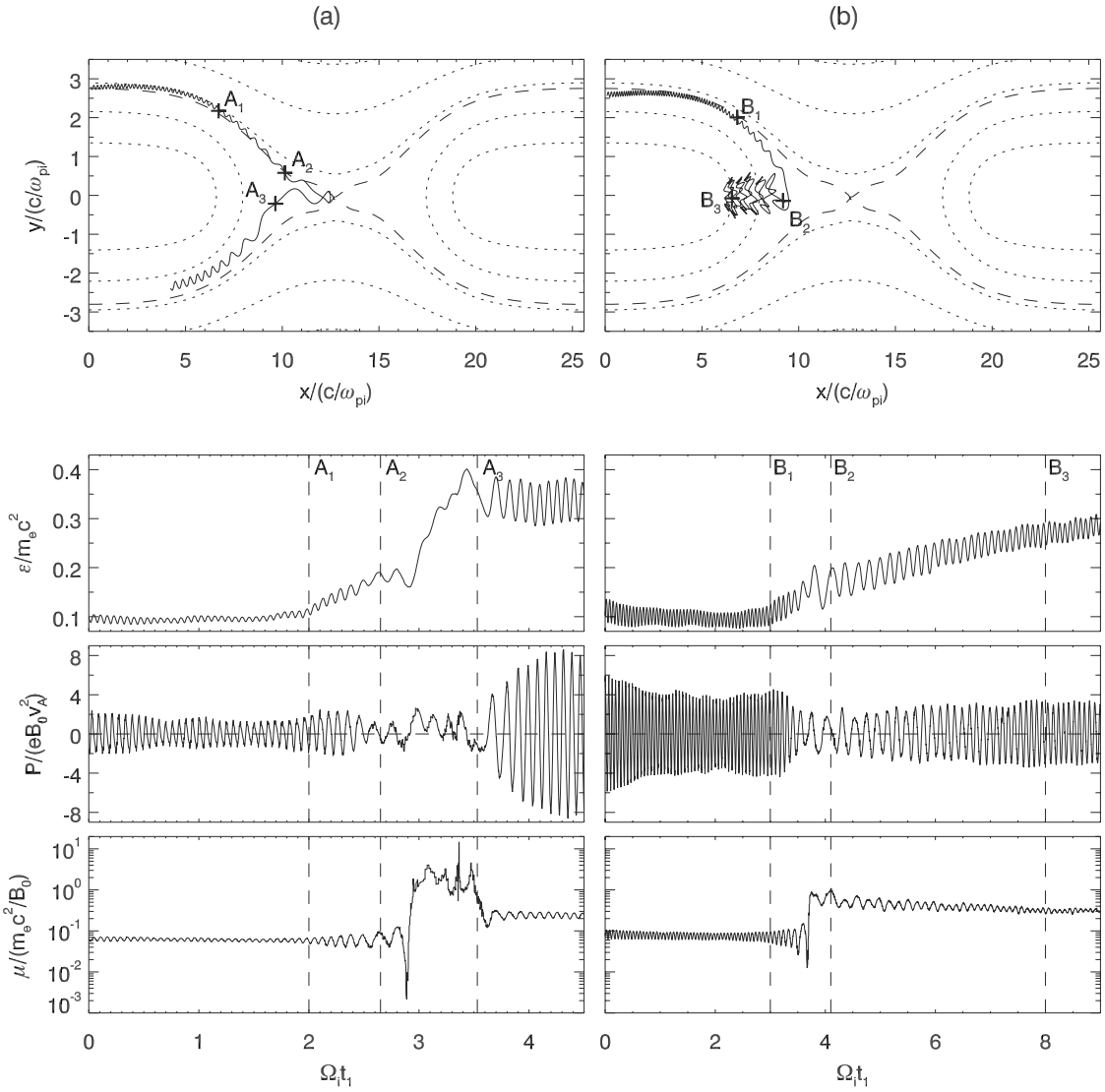

FIG. 9. The evolution of the trajectory, energy ε, power P exerted by the electric field, and the magnetic moment μ for two typical electrons in the antiparallel reconnection. The initial positions of the two electrons are at (a) $x=0.1c/\omega_{pi}$, $y=2.8c/\omega_{pi}$, and (b) $x=0.1c/\omega_{pi}$, $y=2.56c/\omega_{pi}$. The time t_1 is measured from $\Omega_i t=27$, when the fixed electric and magnetic field are taken.

along the z direction. Then because of the electron gyromotion in the magnetic field, the electron distributions have a beam along the x direction in the pileup region (denoted by C_0). In the region inside the negative separatrix (denoted by D_0), the superthermal electrons flow away from the X line can be observed. Figure 5 plots 2D electron velocity distributions $f(v_x,v_y)$ and $f(v_x,v_z)$ at different regions in the guide field reconnection. The arrows in the figure show the directions of the local magnetic field. The results in (a)–(f) are obtained from the regions A_1-F_1 denoted in Fig. 3(b). Electrons are accelerated by the parallel electric field in the region along the negative separatrix (denoted by A_1), and they are directed toward the X lines along the magnetic field lines. The parallel electric field $\mathbf{E}\cdot\mathbf{B}/B$ at $\Omega_i t=29$ in the guide field reconnection is depicted in Fig. 6, and obvious parallel electric field along the pair of the negative separatrix can be found. These electrons are further accelerated by the reconnection electric field in the vicinity of the X line (denoted by B_1), and form a beam along the z direction. In the pileup region (denoted by C_1), there is an electron beam directed along the x direction. In the region just inside the negative separatrix (denoted by D_1), there are two electron beams: one is away from the X line (antiparallel to the magnetic field lines), and the other is directed toward the X line (parallel to the magnetic field lines). In the region along the positive separatrix (denoted by E_1), there is also an electron beam directed toward the X line with speed smaller than in the region along the negative separatrix (denoted by A_1). At the same time, in the region just inside the positive separatrix (denoted by F_1), there is also one electron beam directed away from the X line (antiparallel to the magnetic field lines).

We further investigate electron dynamics in the antiparallel and guide field reconnection by tracing typical electron trajectories. In order to illustrate the acceleration process more clearly, we firstly obtain the electric and magnetic field at a fixed time from the PIC simulations, and then follow the electron trajectories in the fixed electric and magnetic field. The electric and magnetic field is fixed at $\Omega_i t=27$ and $\Omega_i t=29$ in the antiparallel and guide field reconnection, re-

Downloaded 27 Jul 2010 to 211.86.159.15. Redistribution subject to AIP license or copyright; see http://pop.aip.org/pop/copyright.jsp

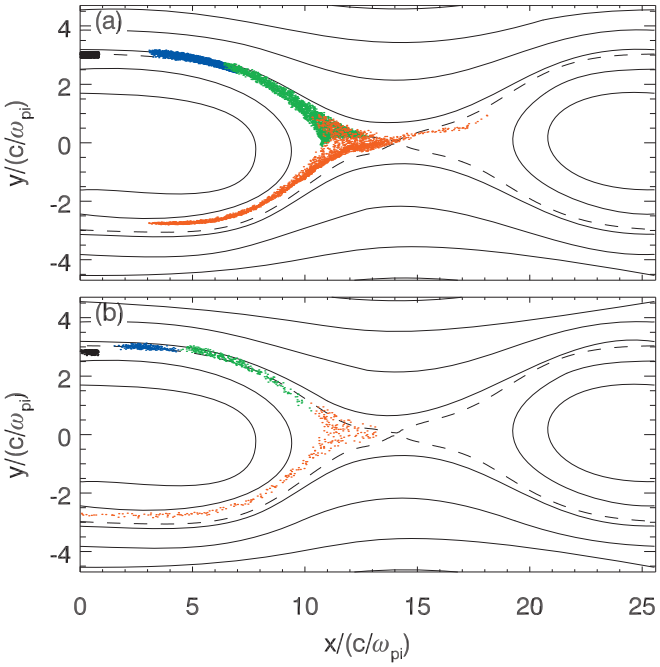

FIG. 10. (Color) The positions of test electrons at different times in the guide field reconnection, and the initial kinetic energy of the electrons is $0.1m_ec^2$. (a) Initially, the test electrons are located in the region $0<x<0.8c/\omega_{pe}$, $2.9c/\omega_{pi}<y<3.1c/\omega_{pi}$, just outside of the separatrix. The different color of the dots represents the positions of test electrons at different times. Black, blue, green, and red dots describe the positions of the test electrons at $\Omega_i t_1=0$, 1.1, 2.2, and 3.3, respectively. (b) Initially, the test electrons are located in the region $0<x<0.8c/\omega_{pe}$, $2.7c/\omega_{pi}<y<2.9c/\omega_{pi}$, just inside of the separatrix. The different color of the dots represents the positions of test electrons at different times. Black, blue, green and red dots describe the positions of the test electrons at $\Omega_i t_1=0$, 2, 4, and 6, respectively. In the figure, only the particles with kinetic energy $\varepsilon>0.3m_ec^2$ are plotted, except for the particles in the initial time. The time t_2 is measured from $\Omega_i t=29$, when the fixed electric and magnetic field are taken.

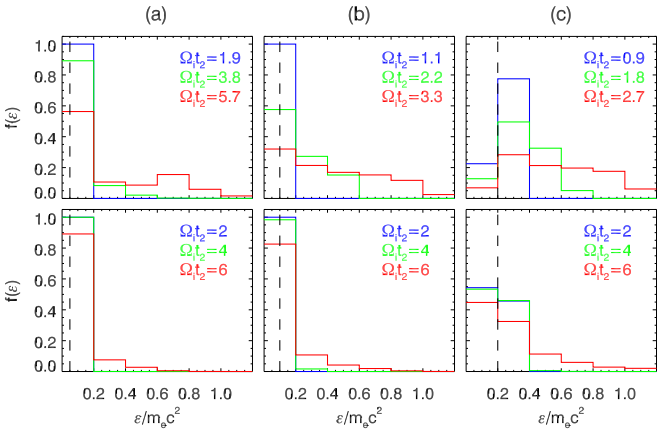

FIG. 11. (Color online) The electron energy distributions at different times in the guide field reconnection. In the top panel, the initial positions of the test electrons are located at the region $0<x<0.8c/\omega_{pe}$, $2.9c/\omega_{pi}<y<3.1c/\omega_{pi}$, just outside of the separatrix. In the bottom panel, the initial positions of the test electrons are located at the region $0<x<0.8c/\omega_{pe}$, $2.7c/\omega_{pi}<y<2.9c/\omega_{pi}$, just inside of the separatrix. (a), (b), and (c) represent the different electron energy, which are $0.05m_ec^2$, $0.1m_ec^2$, and $0.2m_ec^2$, respectively. In the figure, the initial kinetic energies are described with dashed lines, The time t_1 is measured from $\Omega_i t=29$, when the fixed electric and magnetic field are taken.

spectively, when the processes of the two cases are both in the typical growth stage. In the calculations, we have already eliminated the particles moving outside of the boundaries. Figure 7 describes the electron positions at different times in the antiparallel reconnection. In Fig. 7(a), the initial positions of the electrons are just outside of the separatrix, while in Fig. 7(b) the initial positions of the electrons are just inside the separatrix. Initially, all electrons have the same energy $\varepsilon/m_ec^2=0.1$, and they are assumed to have a shell distribution. At first, the electrons move toward the X line along the magnetic field lines. However, the electrons, whose initial positions are outside of the separatrix, can reach the vicinity of the X line. They are then accelerated by the reconnection electric field, and leave the vicinity of the X line along the magnetic field lines just inside of the separatrices. The electrons, whose initial positions are inside of the separatrix, will arrive in the pileup region with the strong magnetic field. Because in the pileup region the curvature radii of the magnetic field lines are very small and comparable to the gyroradii of the energetic electrons, the motions of these energetic electrons are nonadiabatic. They are accelerated to higher energy in the pileup region, and simultaneously move toward $-x$ direction.

Figure 8 shows the evolution of the energy distributions for the electrons with different initial energy in the antiparallel reconnection. In the figure, the top row describes the electrons whose initial positions are outside of the separatrix, while the bottom row is for the electrons whose initial positions are inside of the separatrix. Figures 8(a)–8(c) plot the evolution of the energy distributions for electrons whose initial energy is $\varepsilon/m_ec^2=0.05$, 0.1, and 0.2, respectively. The colors of the dots roughly represent the positions of the electrons: red dots are in the vicinity of the X line, while blue and green dots are in the region near the separatrix, as shown in Fig. 7. For the electrons with initial positions outside of the separatrix, their dominant acceleration occurs in the vicinity of X line, while the electrons whose initial positions inside of the separatrix are accelerated mainly in the pileup region. In general, the efficiency of the electron acceleration is higher in the vicinity of the X line than in the pileup region. However, the electrons can also been preaccelerated when they move toward the X line along the magnetic field lines. The efficiency of the electron acceleration is enhanced with the increase of their initial energy in both the vicinity of the X line and pileup region. The above conclusions can be demonstrated more clearly by following two typical electron trajectories. Figure 9 shows the evolution of trajectory, energy ε, power $P=\mathbf{v}\cdot\mathbf{E}$ exerted by the electric field, and magnetic moment $\mu=m_ev_\perp^2/2B$ of two typical electrons in the antiparallel reconnection. Figure 9(a) describes the electron trajectory whose initial position is outside of the separatrix, while Fig. 9(b) plots the electron trajectory whose initial position is inside the separatrix. For the electron whose initial position outside of the separatrix, it is accelerated mainly in the vicinity of the X line and then leave the region along the magnetic field lines. For the electron whose initial position inside the separatrix, its dominant acceleration is in the pileup region, and its motions are nonadiabatic.

Figure 10 describes the electron positions at different

Downloaded 27 Jul 2010 to 211.86.159.15. Redistribution subject to AIP license or copyright; see http://pop.aip.org/pop/copyright.jsp

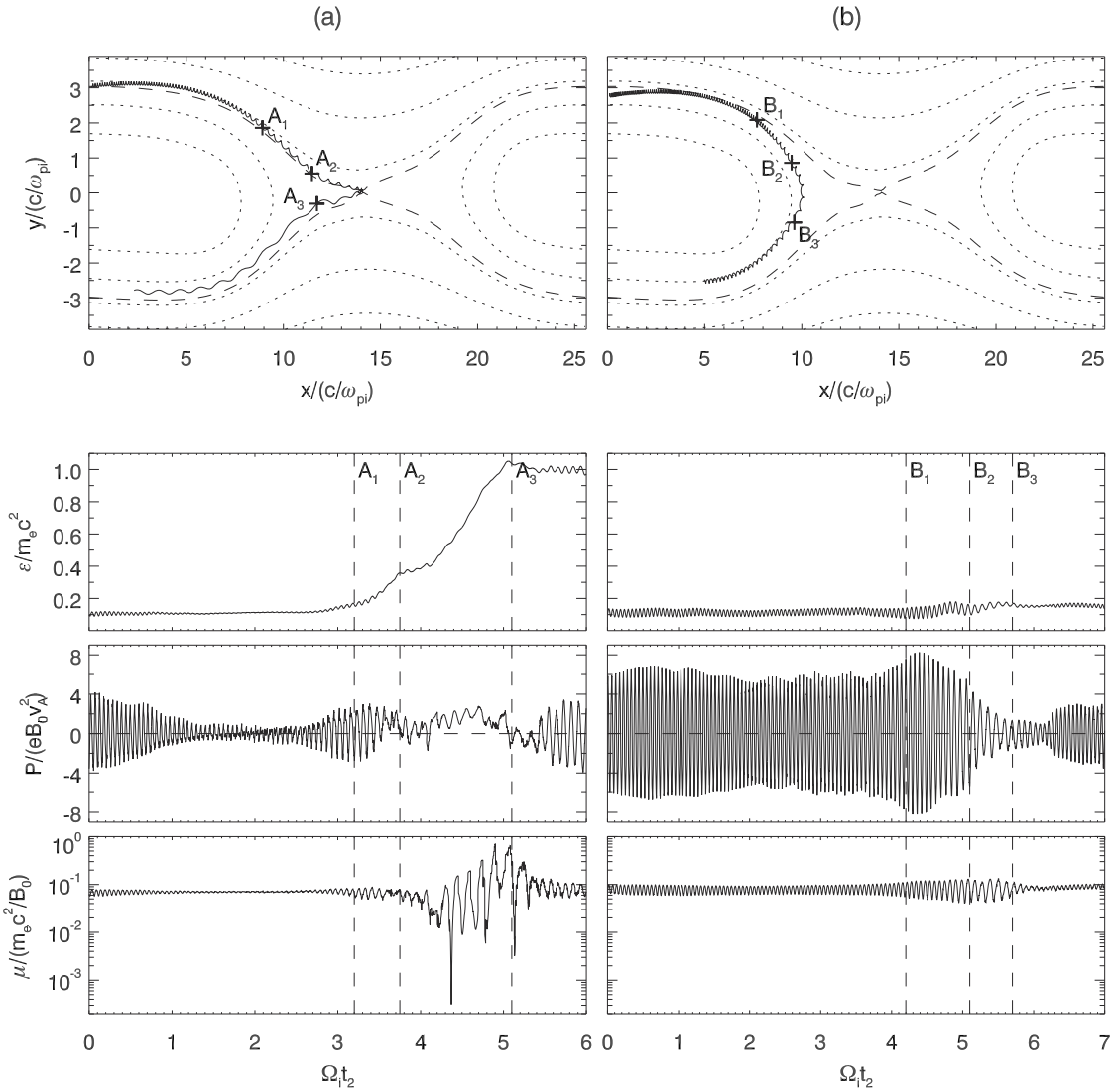

FIG. 12. The evolution of the trajectory, energy ε, power P exerted by the electric field, and the magnetic moment μ for two typical electrons in the antiparallel reconnection. The initial positions of the two electrons are at (a) $x=0.1c/\omega_{pi}$, $y=3c/\omega_{pi}$, and (b) $x=0.1c/\omega_{pi}$, $y=2.75c/\omega_{pi}$. The time t_2 is measured from $\Omega_i t=29$, when the fixed electric and magnetic field are taken.

times in the guide field reconnection. In Fig. 10(a), the initial positions of the electrons are just outside of the separatrix, while in Fig. 10(b) the initial positions of the electrons are just inside the separatrix. Initially, all electrons have the same energy $\varepsilon/m_e c^2=0.1$, and they are assumed to have a shell distribution. In the figure, we have already eliminated the electrons which cross the boundaries. Although the electrons can also be accelerated when they move toward the X line along the magnetic field lines, the dominant acceleration still occurs in the vicinity of the X line. Different from the case of the antiparallel reconnection, the electrons cannot be accelerated in the pileup region. Because the magnetic field in the pileup region is sufficiently strong, the electron gyroradii are much smaller than the curvature radii of the magnetic field lines, and its motions are almost adiabatic.

Figure 11 shows the evolution of the energy distributions for the electrons with different initial energy in the guide field reconnection. In the figure, the top row describes the electrons whose initial positions are outside of the negative separatrix, while the bottom row is for the electrons whose initial positions are inside the negative separatrix. Figures 10(a)–10(c) plot the electrons whose initial energy is $\varepsilon/m_e c^2=0.05$, 0.1 and 0.2, respectively. The colors of the dots roughly represent the positions of the electrons: red dots are in the vicinity of the X line, while blue and green dots are in the region near the separatrix, as shown in Fig. 9. For the electrons with initial positions outside of the negative separatrix, the electrons can be accelerated both along the negative separatrix and in the vicinity of the X line. Therefore, they can be accelerated to much higher energy than in the antiparallel reconnection. For the electrons whose initial positions inside of the negative separatrix, only the electrons reach the vicinity of the X line can be accelerated, therefore the efficiency of electron acceleration is much lower than the electrons whose initial positions are outside the negative separatrix. It can also be found that the electrons are easier to be accelerated to higher energy with the increase of their initial energy. Figure 12 shows the evolution of trajectory, energy ε, power $P=\mathbf{v}\cdot\mathbf{E}$ exerted by the electric field, and magnetic moment $\mu=m_e v_\perp^2/2B$ of two typical electrons in

Downloaded 27 Jul 2010 to 211.86.159.15. Redistribution subject to AIP license or copyright; see http://pop.aip.org/pop/copyright.jsp

the guide field reconnection. Figure 12(a) describes the electron trajectory whose initial position is outside of the negative separatrix, while Fig. 12(b) plots the electron trajectory whose initial position is inside the negative separatrix. The electron whose initial position is outside of the negative separatrix can be accelerated effectively when it moves toward the X line along the magnetic field lines as well as in the vicinity of the X line. For the electron whose initial position is inside the negative separatrix, it cannot be accelerated to high energy because it does not pass through the vicinity of the X line. In the above test particle calculations of the guide field reconnection, we do not find the electron acceleration of the electrons around the pair of the positive separatrices. The electrons around the pair of the positive separatrices are hard to be accelerated because there is no obvious parallel electric field in this region (not shown).

From the above calculations, we can find that a process of an accelerated electron has three stages: flowing into the vicinity of the X line, acceleration in the vicinity of the X line, and flowing out of the vicinity of the X line. In general, every stage lasts less than several ion gyroperiods, which is much smaller than the process of the magnetic reconnection. Therefore, a fixed snapshot will not change our conclusions on the mechanisms of electron acceleration.

IV. DISCUSSION AND CONCLUSIONS

There are numerous evidences of energetic electrons in magnetic reconnection,[15,19,25,26] and these energetic electrons are considered to be accelerated by the reconnection electric field. In this paper, 2D PIC simulations are performed to investigate electron dynamics in antiparallel and guide field reconnection, and we compare the mechanism of electron acceleration in antiparallel and guide field reconnection.

Hoshino *et al.*[28] pointed out that the process of electron acceleration in antiparallel reconnection has two stages: the first is in the vicinity of the X line, and the second in the pileup region. In this paper, we find that electrons can be accelerated both in the vicinity of the X line and the pileup region by the reconnection electric field. Most of the electrons accelerated in the vicinity of the X line come from the region just outside of the separatrices, while most of the electrons accelerated in the pileup region come from the region inside of the separatrices. However, most of the energetic electrons can be accelerated once, in the vicinity of the X line, or in the pileup region. The efficiency of electron acceleration is higher in the vicinity of the X line than in the pileup region.

In guide field reconnection, electrons can be accelerated by the parallel electric field in the vicinity of the X line, as well as when they move toward the X line, which is consistent with Pritchett *et al.*[32] However, we further find that most of these energetic electrons come from the region outside of the negative separatrices. The efficiency of such an acceleration mechanism is obviously higher than that in the antiparallel reconnection, and in both cases the mechanisms of electron acceleration favor the electrons with higher initial energy.

ACKNOWLEDGMENTS

This work was supported by Chinese Academy of Sciences Grant No. KJCX2-YW-N28, the National Science Foundation of China (NSFC) under Grant Nos. 40725013, 40974081, and 40931053, and the Specialized Research Fund for State Key Laboratories.

[1] P. A. Sweet, in *Electromagnetic Phenomena in Cosmical Physics*, edited by B. Lehnert (Cambridge University Press, New York, 1957), p. 123.
[2] E. N. Parker, J. Geophys. Res. **62**, 509, doi:10.1029/JZ062i004p00509 (1957).
[3] V. M. Vasyliunas, Rev. Geophys. Space Phys. **13**, 303, doi:10.1029/RG013i001p00303 (1975).
[4] D. Biskamp, in *Magnetic Reconnection in Plasmas*, edited by M. G. Haines and K. I. Hopcraft (Cambridge University Press, Cambridge, 2000).
[5] E. Priest and T. Forbes, *Magnetic Reconnection: MHD Theory and Applications* (Cambridge University Press, Cambridge, 2000).
[6] J. Birn, J. F. Drake, M. A. Shay, B. N. Rogers, R. E. Denton, M. Hesse, M. Kuznetsova, Z. W. Ma, A. Bhattacharjee, A. Otto, and P. L. Pritchett, J. Geophys. Res. **106**, 3715, doi:10.1029/1999JA900449 (2001).
[7] A. Nishida, *Geomagnetic Diagnostics of the Magnetosphere* (Springer-Verlag, New York, 1978).
[8] P. Ulmschneider, E. R. Priest, and R. Rosner, in *Mechanisms of Chromospheric and Coronal Heating*, edited by R. Rosner (Springer-Verlag, Berlin, 1991).
[9] S. Tsuneta, H. Hara, T. Shimizu, L. W. Acton, K. T. Strong, H. S. Hudson, and Y. Ogawara, Publ. Astron. Soc. Jpn. **44**, L63 (1992).
[10] W. J. Hughes, in *Introduction to Space Physics*, edited by M. G. Kivelson and C. T. Russell (Cambridge University Press, New York, 1995), p. 227.
[11] P. J. Cargill and J. A. Klimchuk, Astrophys. J. **478**, 799 (1997).
[12] J. B. Cao, Y. D. Ma, G. Parks, H. Reme, I. Dandouras, R. Nakamura, T. L. Zhang, Q. Zong, E. Lucek, C. M. Carr, Z. X. Liu, and G. C. Zhou, J. Geophys. Res. **111**, A04206, doi:10.1029/2005JA011322 (2006).
[13] P. L. Pritchett, J. Geophys. Res. **106**, 3798 (2001).
[14] Z. W. Ma and A. Bhattacharjee, J. Geophys. Res. **106**, 3773, doi:10.1029/1999JA001004 (2001).
[15] M. Øieroset, R. P. Lin, T. D. Phan, D. E. Larson, and S. D. Bale, Phys. Rev. Lett. **89**, 195001 (2002).
[16] X. R. Fu, Q. M. Lu, and S. Wang, Phys. Plasmas **13**, 012309 (2006).
[17] P. L. Pritchett and F. V. Coroniti, J. Geophys. Res. **109**, A01220, doi:10.1029/2003JA009999 (2004).
[18] W. G. Wan, G. Lapenta, and G. L. Delzanno, Phys. Plasmas **15**, 032903 (2008).
[19] R. P. Lin and H. S. Hudson, Sol. Phys. **17**, 412 (1971).
[20] R. P. Lin and H. S. Hudson, Sol. Phys. **50**, 153 (1976).
[21] J. A. Miller, P. J. Cargill, A. Emslie, G. D. Holamn, B. R. Dennis, T. N. Larosa, R. M. Winglee, S. G. Benka, and S. Tsuneta, J. Geophys. Res. **102**, 14631, doi:10.1029/97JA00976 (1997).
[22] D. N. Baker and E. C. Stone, Geophys. Res. Lett. **3**, 557, doi:10.1029/GL003i009p00557 (1976).
[23] D. N. Baker and E. C. Stone, J. Geophys. Res. **82**, 1532, doi:10.1029/JA082i010p01532 (1977).
[24] Y. S. Ge and C. T. Russell, Geophys. Res. Lett. **33**, L02101, doi:10.1029/2005GL024574 (2006).
[25] R. S. Wang, Q. M. Lu, C. Huang, and S. Wang, J. Geophys. Res. **115**, A01209, doi:10.1029/2009JA014553 (2010).
[26] R. S. Wang, Q. M. Lu, A. M. Du, and S. Wang, Phys. Rev. Lett. **104**, 175003 (2010).
[27] P. V. Savrukhin, Phys. Rev. Lett. **86**, 3036 (2001).
[28] M. Hoshino, T. Mukai, T. Terasawa, and I. Shinohara, J. Geophys. Res. **106**, 25,979, doi:10.1029/2001JA900052 (2001).
[29] M. Hoshino, J. Geophys. Res. **110**, A10215, doi:10.1029/2005JA011229 (2005).
[30] P. L. Pritchett, Geophys. Res. Lett. **33**, L13104, doi:10.1029/2005GL025267 (2006).
[31] P. L. Pritchett, J. Geophys. Res. **111**, A10212, doi:10.1029/2006JA011793 (2006).
[32] J. F. Drake, M. Swisdak, H. Che, and M. A. Shay, Nature (London) **443**, 553 (2006).

Downloaded 27 Jul 2010 to 211.86.159.15. Redistribution subject to AIP license or copyright; see http://pop.aip.org/pop/copyright.jsp